

Pharmaceutical Nanotechnology

Enhanced antisense effect of modified PNAs delivered through functional PMMA microspheres

Laura Chiarantini^{a,*}, Aurora Cerasi^a, Enrico Millo^b, Katia Sparnacci^c,
Michele Laus^c, Massimo Riccio^d, Spartaco Santi^d, Marco Ballestri^e,
Silvia Spaccasassi^e, Luisa Tondelli^e

^a Institute of Biological Chemistry, University of Urbino, Italy

^b Department of Experimental Medicine, Biochemistry Section, University of Genoa, Italy

^c Department of Environmental and Life Science, University of Eastern Piemonte, Alessandria, Italy

^d ITOI, Consiglio Nazionale delle Ricerche, Bologna, Italy

^e ISOF, Consiglio Nazionale delle Ricerche, Bologna, Italy

Received 4 March 2006; received in revised form 3 July 2006; accepted 6 July 2006

Available online 10 July 2006

Abstract

Peptide nucleic acids (PNA) are very promising antisense agents, but their *in vivo* application is often hampered by their low bioavailability, mainly due to their limited uptake through cellular and nuclear membranes. However, PNA chemical synthesis easily allows modification with functional structures able to improve the intrinsically low permeability and great interest is arising in finding specific and efficient delivery protocols. Polymeric core-shell microspheres with anionic functional groups on the surface were tested for their ability to reversibly bind lysine modified PNA sequences, whose antisense activity against COX-2 mRNA was already demonstrated in murine macrophages.
© 2006 Elsevier B.V. All rights reserved.

Keywords: Peptide nucleic acids (PNA); Core-shell microspheres; Cyclooxygenase-2 (COX-2); PMMA microspheres; Macrophages; Antisense therapy

1. Introduction

Peptide nucleic acids (PNA) are synthetic mimics of DNA in which the deoxyribose phosphate backbone is replaced by repeating *N*-(2-aminoethyl)-glycine units to which the nucleobases are attached via a methyl carbonyl linker (Nielsen *et al.*, 1991). Due to the uncharged and flexible polyamide backbone, PNAs display an increased binding affinity for complementary sequences and biostability against nucleases and proteases while retaining the specificity of Watson and Crick recognition (Demidov *et al.*, 1994; Albertshofer *et al.*, 2005). An additional consequence of the polyamide backbone is that PNAs hybridize virtually independently of the salt concentration. Thus the thermal stability of PNA/DNA duplexes is barely affected by low ionic strength. In contrast to DNA, PNA can bind in either parallel or antiparallel manner, being the latter the more favored orientation. Finally, PNA/RNA hybridization is sig-

nificantly more affected by base mismatches with respect to DNA/RNA duplexes. The absence of a charged backbone also prevents PNAs from binding to proteins that normally recognize polyanions, removing a major source of non-specific interactions (Hamilton, 1996). These properties, together with lack of toxicity at even relatively high concentrations, suggested that PNA should be considered as highly promising compounds for antisense applications. However, as PNAs are large uncharged molecules (typically 3000–4000 MW), it is not surprising that they are taken up very poorly by eukaryotic and prokaryotic cells (Koppelhus and Nielsen, 2003). In addition, small amount of PNA that is internalized inside the cells, often seems to remain trapped in vesicular structures, thus resulting in a reduced bioavailability.

Even if there is no general consensus about the uptake of unmodified PNAs by mammalian cells, it seems to be cell-type dependent and different from the mechanism employed by charged oligonucleotides. Despite their limited diffusion through cellular and nuclear membrane, PNAs high chemical versatility allows their conjugation with structures that improve

* Corresponding author. Tel.: +39 0722305220; fax: +39 0722320188.
E-mail address: l.chiarantini@uniurb.it (L. Chiarantini).

Table 1
Synthesized PNA sequences

PNA	Sequence	MW (g/mol)
AS KKK-A25	2HN-Lys-Lys-Lys-GCCCCAGGGCAGCGCA-CONH ₂	4734.0
AS KKK-A25 Rhod	RHOD-GCCCCAGGGCAGCGCA-Lys-Lys-Lys-CONH ₂	5059.0
AS A25	2HN-GCCCCAGGGCAGCGCA-CONH ₂	4349.5
Scr A25	2HN-Lys-Lys-Lys-AGCGCGGACGCGACCC-CONH ₂	4734.0
AS KKK-S3	2HN-Lys-Lys-Lys-GGAAGAGCATCGCAGA-CONH ₂	4820.0
Scr S3	H2N-Lys-Lys-Lys-GGCGCAAGACGGTAA-CONH ₂	4820.0
AS KKK-L205	2HN-Lys-Lys-Lys-ATTCCCCACGGTTT-CONH ₂	4122.3
Scr L205	2HN-Lys-Lys-Lys-CCATCACTCGTTGT-CONH ₂	4122.3

the intrinsically low permeability. Therefore, faster progress in the development of PNA as therapeutic agents depends on finding efficient and specific delivery protocols.

Several methods have been devised in the past years to address this issue, including electroporation (Shammas et al., 1999), use of pore-forming agents (Faruqi et al., 1998), scrape delivery (Sazani et al., 2001), loaded red blood cells (Chiarantini et al., 2002) and cationic liposomes (Hamilton et al., 1999). An alternative approach is represented by functional polymeric microspheres able to reversibly adsorb biomolecules on their surface. We previously demonstrated that plasmid DNA and proteins can be delivered through specifically designed core-shell microspheres (Caputo et al., 2004; Ensoli et al., 2004). In addition, ionic interaction of nucleic acids with biocompatible cationic microspheres results in increased cellular uptake and intracellular stability (Tondelli et al., 1998).

Ionic interaction with specifically designed functional core-shell microspheres can also be achieved with PNA sequences once they are modified with a few acid or basic aminoacids at one end in order to be able to spontaneously associate with cationic or anionic particles, respectively. It is well known that terminal modifications of PNA sequences by aminoacids, oligopeptides or peptides do not significantly affect their biological activity (Koppelhus et al., 2002; Turner et al., 2005; Scarfi et al., 1997). Therefore, we here propose the design and synthesis of several biological active PNAs modified with three lysine units at the amino terminal.

These cationic PNAs can be further adsorbed onto carboxylated poly(methylmethacrylate) (PMMA) core-shell microspheres (H1D4) obtained by dispersion polymerization of methylmethacrylate in the presence of commercial Eudragit L100-55 stabilizer (Sparnacci et al., 2005). We previously described the specific biological activity of native and modified antisense PNAs (Chiarantini et al., 2005a,b; Scarfi et al., 2003) directed against cyclooxygenase (COX), the prostaglandin endoperoxide synthase, the key enzyme responsible for the conversion of arachidonic acid to prostaglandins. At least two isoforms of cyclooxygenase being identified: COX-1 which is constitutively expressed and COX-2 which is highly inducible by growth factors, cytokines and tumor promoters (Smith et al., 1996; Dubois et al., 1998). COX-2 is localized at inflammatory sites and neoplastic tissues and is implicated in processes of the diseases while COX-1 is likely to synthesize prostaglandins (PGs) that regulate homeostatic functions (Dubois et al., 1998;

Vane et al., 1998). Traditional non-steroidal anti-inflammatory drugs (NSAIDs) inhibit both enzymes whereas the new class of COX-2 selective acts as inhibitor of COX-2. Interestingly, epidemiological studies showed a 40–50% reduction in death related to colorectal cancer in individuals taking NSAIDs (Smalley and DuBios, 1997; Sheehan et al., 1999). To explain this observation, overexpression of COX-2 is detected in many human tumors including gastric cancer (Hida et al., 1998; Leung et al., 2003). Glucocorticoids, on the other hand, suppress COX-2 expression potently (Crofford et al., 1994) although continuous use of the agents is often limited by their own side effects. Antisense PNAs (AS PNAs) represent a powerful tool for specific inhibition of gene expression at the mRNA level (Putnam, 1996). Several modified PNAs directed against COX-2 mRNA can be used as a proof of concept to investigate the ability of core-shell microspheres to efficiently deliver antisense molecules in a murine macrophage model.

2. Materials and methods

2.1. Materials

4-Methyl-benzoydryl-amine-(MBHA) resin, *O*-(7-azabenzotriazol-1-yl)-1,1,3,3 tetramethyl-uronium hexafluorophosphate (HATU), *N,N*-diisopropylethylamine (DIEA), *N*-methylpyrrolidone (NMP), acetic anhydride, sim-collidine, trifluoromethanesulfonic acid (TFMSA), Rhodamine B (Rhod) were of reagent grade. *N,N* dimethylformamide, diethyl ether, acetonitrile, *m*-cresol were obtained from commercial sources and used without further purification unless indicated.

2.2. PNA synthesis and purification

KKK-S3 and KKK-A25 16mer antisense PNAs and L205 14 mer antisense PNA (Table 1), complementary to the regions 119–134, 149–164 and 105–118 of murine COX-2 cDNA (GeneBank accession number M64291), respectively, were synthesized and chemically modified by the introduction of a lysinic tripeptide moiety at the amino-terminal. Three lysine modified scramble PNAs were obtained. Moreover, A25 sequence without terminal modification was also prepared. In addition, KKK-A25 PNA sequence was also labelled by direct coupling of Rhodamine B on the solid support to the amino terminal of the protected PNA sequences (Table 1).

All PNA-sequence molecules were manually synthesized introducing minor modifications in the standard method of solid phase peptide synthesis which follows the *tert*-butoxycarbonyl (Boc) strategy (Christensen et al., 1995): 100 mg of MBHA resin (1.1 mmol/g) were downloaded with the first PNA monomer (0.024 mmol) in the presence of 0.02 mmol of HATU as coupling reagent, 0.048 mmol of DIEA as base in *N*-methylpyrrolidone. Capping after first monomer loading was carried out with a mixture of acetic anhydride-sim-collidine-*N,N* dimethylformamide (8.9/0.6/0.5, v/v/v). The PNA sequence elongation was then performed using the following conditions:

- (a) *deprotection* in a mixture of trifluoroacetic acid/*m*-cresol (95/5, v/v);
- (b) *coupling* in a mixture containing five equivalents (equiv.) of Boc-PNA monomer or of Boc-Lys (2-Cl-Z)-OH 4.5 equiv. of HATU, 5.0 equiv. of DIEA, 7.5 equiv. of sim-collidine at 0.1 M monomer (or amino acid) final concentration in anhydrous NMP;
- (c) *capping* in a mixture of acetic anhydride-sim-collidine-*N,N* dimethylformamide (8.9/0.6/0.5, v/v/v).

The same protocol was used to obtain rhodamine PNAs using a coupling mixture containing five equivalents of Rhodamine B, 4.5 equiv. of HATU, 5.0 equiv. of DIEA, 7.5 equiv. of sim-collidine at 0.1 M final concentration in anhydrous NMP.

Cleavage of PNA from solid support was carried out by treatment with TFA/TFMSA/*m*-cresol mixture (8/2/1). The solvent was partially evaporated and the product precipitated with ice cold diethyl ether. All PNA sequences were purified by reverse phase high performance chromatography (RP-HPLC) on a Shimadzu LC-9A preparative HPLC equipped with a Phenomenex C18 Luna column (21.20 mm × 250 mm). Solvent A was 0.1% TFA in water and solvent B was 0.1% TFA in acetonitrile. The solvent program was a gradient starting with 100% solvent A for 5 min, linearly increasing to 70% solvent B in 30 min and up to 100% B in 5 min. The diode array detector was set at 260 nm during the analyses. Mass spectra of each PNA sequence was obtained in the positive ion mode using a single quadrupole mass spectrometer (HP Engine 5989-A) equipped with an electrospray ion source (ESI-MS) and confirmed by electrospray iontrap mass spectrometry (ESI-TRAP-MS). After purification, the synthesis had a final yield of 60–70% depending on the type of sequence with a purity of 95% at least after preparative HPLC purification.

2.3. Microspheres preparation and characterization

Core-shell microspheres H1D4 and fluorescent microsphere (H1D-FLUO) were prepared by dispersion polymerization as previously described (Sparnacci et al., 2005). Microsphere size and size distribution were measured using a JEOL JEM 100CX scanning electron microscope (SEM) operating at an accelerating voltage of 20 kV. The samples were sputter coated under vacuum with a thin layer (10–30 Å) of gold. The magnification was given by the scale on the micrograph. The amount of Eudragit L 100-55 linked to the microsphere surface was

determined by back titration of the excess NaOH after complete reaction of the acid groups and microsphere removal by centrifugation. ζ -Potential measurements were carried out at 25 °C on a Malvern Zetasizer 3000 HS instrument, after dilution of microspheres in the presence of 10 mM NaCl solution. All measurements were run in triplicate (\pm S.D. < 15%). Absorption spectra were recorded on a UV Perkin-Elmer Lambda20 spectrophotometer (λ = 260 nm).

2.4. PNA/microsphere complex preparation

A 10.0 mg of microspheres were incubated in 1.0 ml of a 20 mM sodium phosphate buffer at pH 7.4 in the presence of different PNA concentrations (from 10 to 1000 μ g/ml) for 2 h at room temperature. Then, the microspheres were collected by centrifugation in a microfuge at 8000 rpm for 10 min. The supernatant was filtered on low protein binding filter units (Millex GV100 Millipore) and unbound PNA was estimated by UV spectroscopy at 260 nm. Molar extinction coefficients were measured in 20 mM phosphate buffer pH 7.4 for each PNA sequence. The amount of adsorbed PNA was calculated as the difference between the given and the unbound PNA. PNA binding experiments (50 or 250 μ g/ml) to H1D4 microspheres (10 mg/ml) at different ionic strength were run in 20 mM phosphate buffer (pH 7.4) added with increasing salt amount (0–1.0 M NaCl). Similarly, the effect of pH in PNA adsorption experiments was studied in a standard buffer (0.03 M citric acid + 0.03 M potassium phosphate + 0.03 M boric acid) by adding increasing amounts of 0.2 M NaOH aqueous solution. In both cases, incubation was run for 2 h at room temperature and the amount of unbound PNA was detected, after centrifugation and supernatant filtration, as previously described.

For release experiments, previously prepared PNA/microsphere complexes were incubated in the presence of 1 M NaCl + 20 mM phosphate buffer (pH 7.4) for 30 min at 37 °C. After centrifugation in a microfuge at 8000 rpm for 10 min and filtration, the amount of released PNA in the supernatant was estimated by UV spectroscopy at 260 nm.

2.5. Preparation of murine macrophages

Swiss mice were injected with 1.0 ml of 10% thioglycolate (Sigma, USA) intraperitoneally. On day 4, the peritoneal exudate cells were obtained by peritoneal lavage with 10 ml of ice-cold Hank' balanced salt solution supplemented with 10 U/ml of heparin. The cells were washed twice, resuspended in culture medium DMEM (International PBI, Italy) supplemented with 10% heat-inactivated foetal calf serum (FCS), 1% antibiotics, 2 mM glutamine, and overlaid on plastic dishes (35 mm culture plates, Sarstedt, Italy). The plates were incubated in a humidified 5% CO₂ atmosphere at 37 °C over night to allow macrophage adherence. Plates were washed with gentle agitation with warmed DMEM medium for dislodge nonadherent cells, and a macrophage monolayer was obtained. About 95% of the adherent cells were macrophages as determined by immunostaining and surface marker analysis.

2.6. Microspheres cytotoxicity in murine macrophages

Murine macrophages (5×10^5 cells/ml) were incubated with increasing concentrations (0–500 $\mu\text{g/ml}$) of microsphere, alone or bound to PNA. After 24 or 48 h incubation, cell viability was measured by the CellTiter 96[®] AQueous One Solution Cell Proliferation Assay (Promega Corporation, USA) that contains a novel tetrazolium compound [3-(4,5-dimethyl-2-yl)-5-(3-carboxymethoxyphenyl)-2-(4-sulfophenyl)-2H-tetrazolium, inner salt; MTS] and an electron coupling reagent (phenazine ethosulfate; PES). PES has enhanced chemical stability, which allows it to be combined with MTS to form a stable solution. The MTS tetrazolium compound is bioreduced by cells into a colored formazan product that is soluble in tissue culture medium. This conversion is presumably accomplished by NADPH or NADH produced by dehydrogenase enzymes in metabolically active cells. Assays are performed by adding a small amount of the CellTiter 96[®] AQueous One Solution Reagent directly to culture wells, incubating for 4 h and then recording the absorbance at 490 nm with a 96-well plate reader. The quantity of formazan product as measured by the absorbance at 490 nm is directly proportional to the number of living cells in culture. The experiments were run in quadruplicate.

2.7. Microsphere phagocytosis by murine macrophages in vitro

Murine macrophages (3×10^6 cells/ml) were incubated in the presence of microspheres (10 or 50 $\mu\text{g/ml}$) for 1, 2 and 4 h. Cells were extensively washed to remove non-phagocytosed microspheres, fixed with 2% paraformaldehyde and 2.5% glutaraldehyde for 30 min at 4 °C, and stained with toluidine blue. Cells were observed at a phase contrast microscope (100 \times) to count the number of macrophages with phagocytosed microspheres.

2.8. Confocal microscopy

For confocal microscopy analysis, the fluorescent microspheres (H1D-FLUO) coated with rhodamine KKK-PNA obtained as previously described were collected in phosphate buffer at pH 7.4 and were allowed to sediment on a coverslip. The murine macrophages (3×10^6 cells/ml) were incubated for 1, 2, 4, (4+2), (4+4) or (4+20) h in the presence of rhodamine KKK-A25 PNA H1D-FLUO microsphere complexes (10 or 50 $\mu\text{g/ml}$) obtained as previously described. After incubation at 37 °C, 5% CO₂, with macrophages for 2, 20 and 24 h, they were observed at the confocal microscope. The confocal imaging was performed on a Radiance 2000 confocal laser scanning microscope (BioRad), equipped with a Nikon 60 \times , water immersion 1.3 N.A. objective and with a argon–krypton laser. For H1D-FLUO microspheres and KKK-A25 Rhod PNA double detection the samples were sequentially excited with the 488 and 568 nm lines of the argon–krypton laser to minimize the overlapping between the two signals. The emission signals were detected by two photomultiplier tubes. Two barrier filters (BP; 515/30 nm for H1D-FLUO and LP; 600 nm for rhodamine

PNA) were placed before the two photomultiplier tubes as previously described (Riccio et al., 2001). Optical sections were obtained at increments of 0.5 μm in the Z-axis and were digitized with a scanning mode format of 512 \times 512 pixels and 256 grey levels. A phase contrast image was simultaneously collected for real-time living cells detection. Intracellular localization of the fluorescent microspheres was detected only in sections passing through the nuclear interior of living cells. The image processing and the volume rendering were performed using the ImageSpace software (Molecular Dynamics, USA) running on a workstation Silicon Graphics Indigo2 (Mountain View, CA).

2.9. In vitro biological activity

Murine macrophages (3×10^6 /plate) were incubated for 4 h in the presence of PNA-microsphere complexes (10 $\mu\text{g/ml}$). Unphagocytosed complexes were carefully removed by repeated washes and macrophages were maintained in fresh medium for 4 h prior to stimulation in order to complete the uptake of the remaining adhering microspheres. Free microspheres and complexes with scramble PNA sequence (i.e. Scr A25, Scr S3 and Scr L205) were used as negative controls. As specific inhibitor of COX-2 expression NS-398 (*N*-[2-(Cyclohexyloxy)-4-nitrophenyl]methanesulfonamide) (10, 50 and 100 μM) was added to the culture media. Then, macrophages were further incubated for 18 h with or without 50 ng/ml of lipopolysaccharide (LPS) from *Escherichia Coli* (serotype 0111:B4, Sigma Italy) to elicit the expression of COX-2.

After stimulation with LPS, cells were harvested by scraping with a solution containing 50 mM Tris–HCl, pH 7.6, 0.25 M sucrose, 1% (w/v) SDS, 2 $\mu\text{g/ml}$ leupeptin, 1 $\mu\text{g/ml}$ pepstatin, 2 mM phenylmethylsulphonyl fluoride (PMSF), 5 mM ethylenediaminetetraacetic acid (EDTA) and 5 mM *N*-ethylmaleimide. Cellular extracts were immediately boiled for 5 min, sonicated and centrifuged at 14,000 rpm to remove insoluble debris. Protein content was assayed by Lowry's method (Lowry et al., 1951) and 40 μg of protein extracts were resolved on 8% SDS-polyacrylamide gel, transferred to nitrocellulose membranes (Amersham Life Science, UK) and then detected with an antibody specific against COX-2 (M-19, Santa Cruz Biotechnology Inc., USA). The secondary antibody was horseradish peroxidase-conjugated goat anti-rabbit IgG and visualized with the ECL detection kit (Amersham Life Science, UK) according to the manufacture's instruction. Membranes were stripped and reprobed with an antibody against p65 (Rel A) (C-20, Santa Cruz Biothecnology, USA). Immunoreactive bands were quantitated by laser densitometry and COX-2 levels were normalized to p65.

3. Results

Terminally modified PNA sequences, complementary to different regions of murine COX-2 mRNA (Table 1), were synthesized and physico-chemically characterized as described in Section 2. During the synthesis, three lysine aminoacids were added at the amino terminal of three sequences of PNA to facilitate aqueous solubility and to allow reversible interaction with carboxylated core-shell microspheres.

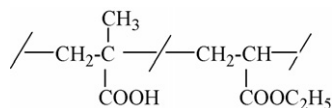


Fig. 1. Chemical structure of Eudragit L100-55.

Poly(methyl methacrylate) core-shell microspheres were prepared by dispersion polymerization. An appropriate selection of the experimental parameters, such as the initiator and stabilizer amount and the medium solvency power, allows the preparation of samples with a narrow size distribution (Spamacci et al., 2005). The resulting microspheres present a core-shell structure in which the inner core is mainly constituted by poly(methylmethacrylate) and the outer shell by the steric stabilizer Eudragit L100-55 (Fig. 1) which has carboxylic groups able to interact with modified PNA with basic aminoacidic residues (i.e. lysine) at physiological pH.

Scanning electron microscope (SEM) analysis of sample H1D4 (Fig. 2) shows a mean diameter of $2.07 \pm 0.12 \mu\text{m}$, whereas titration of surface carboxylic groups indicate a specific charge density of $40.9 \mu\text{mol/g}$ ($=14.2 \mu\text{mol/cm}^2$). At physiological pH, the free microspheres have a net negative charge as confirmed by ζ -potential measurements ($-67.9 \pm 1.2 \text{ mV}$).

The affinity of KKK-A25, KKK-S3 and KKK-L205 PNA sequences for the described microspheres was measured by means of adsorption experiments run in sodium phosphate buffer (20 mM, pH 7.4) at room temperature (Fig. 3). No differences in PNA adsorption amount was detected between the three sequences, which have similar length but different base composition (Table 1).

PNA loading values can be modulated (5–40 $\mu\text{g/mg}$) according to initial PNA concentration (50–500 $\mu\text{g/ml}$), while maintaining good adsorption efficiency (82–97%). This binding is specific for lysine modified PNAs as native antisense A25 PNA fails to bind to H1D4 microspheres under the same experimental conditions (data not shown). In the case of KKK-A25 PNA the isotherm binding curve was tested up to 1 mg/ml PNA concentration thus finding a plateau value of 49 $\mu\text{g/mg}$ of adsorbed PNA, corresponding to approximately 50% binding efficiency. In any case, the eventually unbound PNA can be easily removed

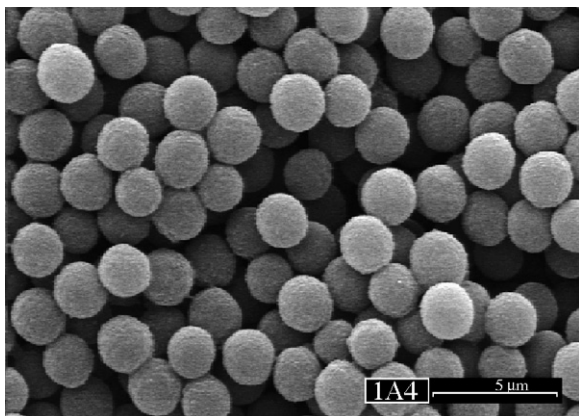


Fig. 2. SEM micrograph of microsphere sample H1D4.

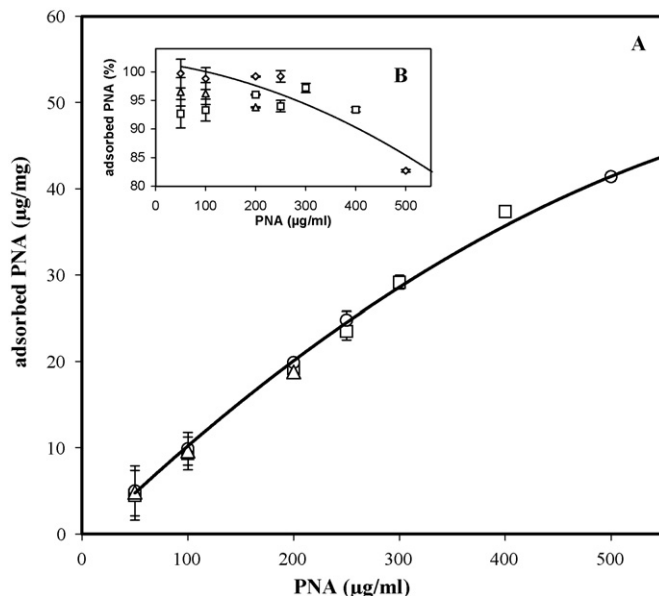


Fig. 3. Panel A: adsorption isotherms of PNAs on H1D4 microspheres. KKK-A25 (empty circle), KKK-S3 (empty square) and KKK-L205 (empty triangle) at physiological pH after 2 h at room temperature in the presence of 10 mg/ml of microspheres H1D4. Panel B: PNA binding efficacy (%). Data are the mean of three different experiments \pm S.D.

upon two separate washing in phosphate buffer. To obtain more information on PNA adsorption mechanism, binding was run in phosphate buffers at different ionic strength (0–1.0 M NaCl) showing maximum adsorption rate at low salt concentration. In the presence of both low and high PNA concentration, binding is favored when run in neutral and basic buffers (Fig. 4).

The interaction between PNA and microspheres is reversible as demonstrated through cell-free experiments with microsphere complexes obtained with different PNA concentrations

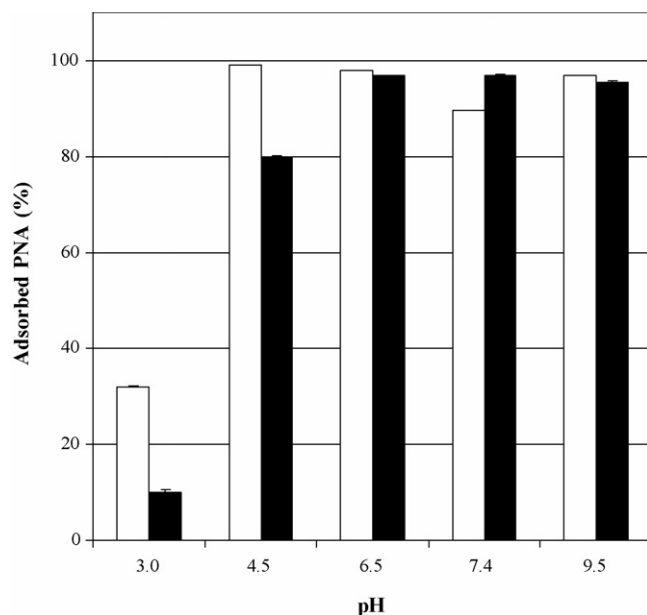


Fig. 4. PNA adsorption vs. pH. KKK-A25 50 $\mu\text{g/ml}$ (white bars); 250 $\mu\text{g/ml}$ (black bars). Data are the mean of three different experiments \pm S.D.

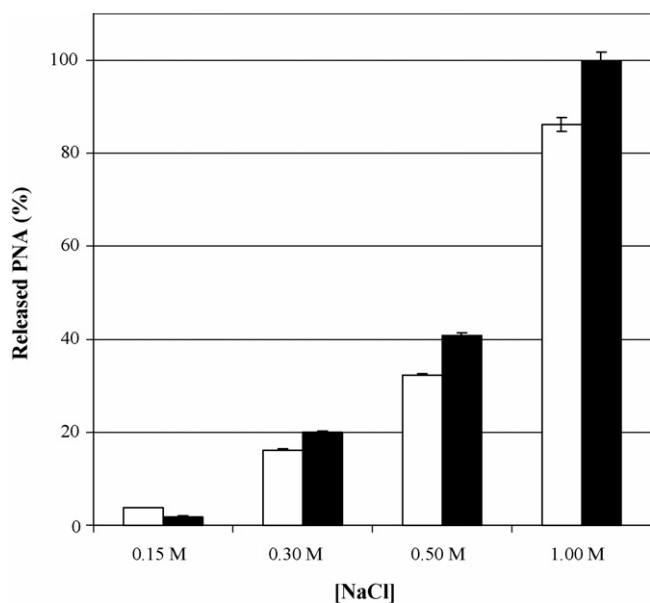


Fig. 5. PNA released at different salt concentration. KKK-A25 50 µg/ml (white bars); 250 µg/ml (black bars). Data are the mean of three different experiments ± S.D.

(50 and 250 µg/ml): PNA release is fast (30 min) and extensive (16–100%) especially in the presence of buffers with high salt concentration (Fig. 5). Moreover, at pH > 4, PNA is most recovered (92–100%) from the samples with the lowest loading value (data not shown), suggesting that modulation of PNA/microsphere complex composition can result in PNA amount controlled release.

The cellular toxicity of free microspheres was investigated in murine macrophages. Our data clearly demonstrate the relatively non-toxic nature of H1D4 microspheres in the time range studied (Fig. 6). When we verified the effect of conjugation with PNA, no significant differences were found if compared with free microspheres (data not shown).

The adsorption of a KKK-PNA onto core-shell microsphere was clearly demonstrated by confocal microscopy (Fig. 7). When macrophages are cultured in the presence of core-shell microspheres, extensive phagocytosis can be seen at a phase contrast microscope, indicating that all particles were taken up at 85–90% after 4 h of exposure. When macrophage were cultured with H1D-FLUO microspheres coated with Rhod KKK-A25 PNA and observed with confocal and fluorescent microscopy

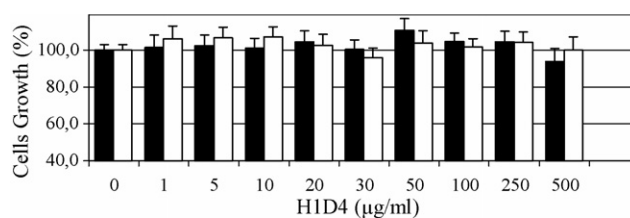


Fig. 6. Macrophage toxicity of H1D4 microspheres. Filled bars: 24 h exposure; empty bars: 48 h exposure. Data are expressed as cell growth percentage to untreated cells. Data are run in quadruplicate and are the mean of two different experiments ± S.D.

the uptake of PNA microsphere complexes was evident (Fig. 8)

To examine the effect of PNA on COX-2 protein expression, murine macrophages were treated with free microspheres or antisense or scramble PNA–microspheres complexes and subsequently stimulated with LPS for 18 h. The cellular extracts were prepared and tested for COX-2 expression by Western blot analyses. The evaluation of COX-2 levels by laser densitometry of the immunoreactive band, normalized to p65 (Rel A) is reported in Fig. 9.

Immunoblot analysis of unstimulated macrophage cellular extracts revealed that no COX-2 expression was detectable (Fig. 9, lane 1). Upon stimulation with LPS, the COX-2 band was visible (lane 2–9) and the phagocytosis of free microspheres (lane 3) or complexed with scramble PNAs (lanes 4, 6 and 8) do not affect the expression of the protein. On the contrary, antisense PNA/microsphere complexes are able to significantly reduce COX-2 expression (lanes 5, 7 and 9) with high efficiency (40% for KKK-A25, 39% for KKK-S3 and 31% for KKK-L205).

4. Discussion

Wider application in inflammatory diseases of peptide nucleic acids as antisense agents appears to be limited by poor cellular uptake in monocytes and macrophages. It is well known that terminal modification of PNAs with a few cationic aminoacids does not hamper their biological activity in vitro and is able to improve their cellular uptake (Sazani et al., 2001). However, specific antisense effect in vitro and in vivo application can be reached only with high doses of PNA sequences (Sazani et al., 2002).

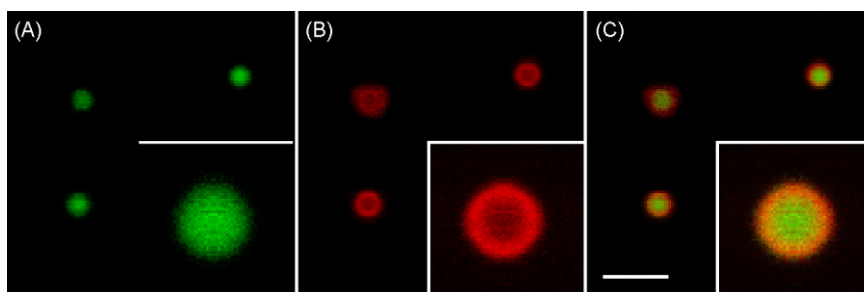


Fig. 7. Confocal microscopy images of fluorescent microspheres (H1D-FLUO) (A) conjugated to rhodamine PNA (Rhod KKK-A25) (B). Merged images (C) show that fluorescent microspheres are coated with rhodamine KKK-PNA. The insets show a single microsphere at three times magnification. Bar = 5 µm.

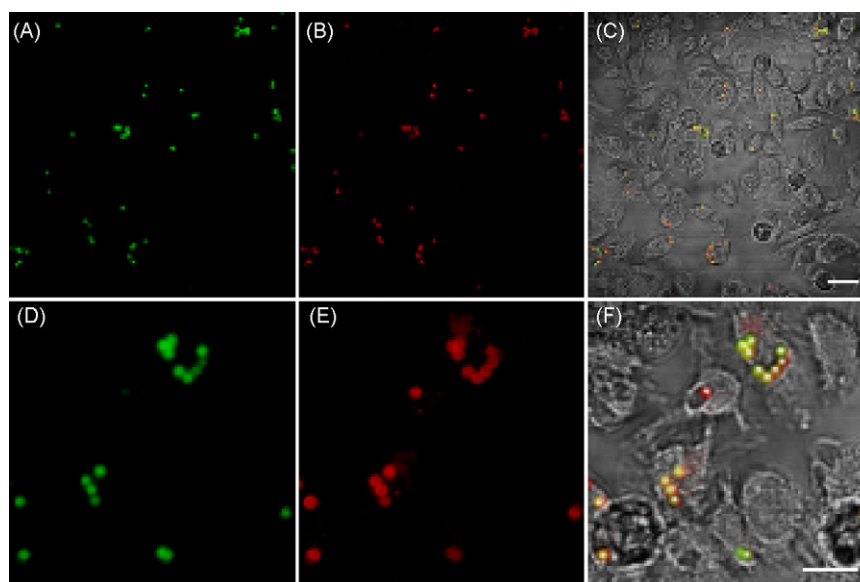


Fig. 8. Confocal microscopy images of the uptake of green HID-FLUO microspheres (A and D) conjugated with red rhodamine KKK-A25 PNA (B and E) when incubated for 4 h with macrophages. Merged images (C and F) are superimposed with phase contrast. Bars = 10 μm .

We here present a promising application of functional polymeric core-shell microspheres for the specific delivery of cationic PNAs. These poly(methylmethacrylate) microspheres were previously tested for protein delivery and vaccine purposes: they are highly biocompatible, not toxic *in vitro* and *in vivo* (Caputo et al., 2004; Sparnacci et al., 2005) and bear ionizable groups on the surface able to establish reversible ionic interactions with charged biomolecules. Their preparation is easy to

scale up and is highly reproducible. In addition, they can be lyophilized alone or complexed with biomolecules without any loss of biological activity (Ensoli et al., 2004).

As a proof of concept, biologically active antisense PNA sequences directed against COX-2 mRNA were prepared with a few lysine units covalently linked at the amino terminal. To test the efficacy of polymeric microspheres as delivery systems, no other significant chemical modification of these PNA sequences was considered (i.e. lipophilic moieties, positively charged peptides such as Antennapedia, nuclear localization signal peptides), as they were often found to play an important role in improving endocytotic uptake or in giving rise to non-specific interactions with cellular proteins (Rapozi et al., 2002).

Lysine modified PNAs were adsorbed on the surface of carboxylated core-shell microspheres in different experimental conditions at physiological pH and the stability of these complexes was elucidated in several physiologically relevant buffers. At physiological pH, PNA interaction with microsphere surface seems mainly driven by the formation of ionic pairs between the lysinic units and the carboxylate functional groups: adsorption rate is favored in low ionic strength buffers and at neutral and basic pH, where the degree of deprotonation of microsphere functional groups is higher. Adsorption efficiency is very high in a wide PNA concentration range, thus allowing a fine modulation of the amount of bound PNA with great reproducibility. Extensive release of intact PNA occurs in the presence of high salt concentration thus demonstrating the reversibility of the interaction. Confocal microscopy shows that PNA is adsorbed on the outer surface of the microspheres and that in the presence of living macrophages PNA/microsphere complexes are actively phagocytosed and able to extensively release PNAs in a time dependent manner.

An important requirement of synthetic delivery systems is the lack of cytotoxicity, which can be affected by their chemical composition, size and size dispersion, surface charge and

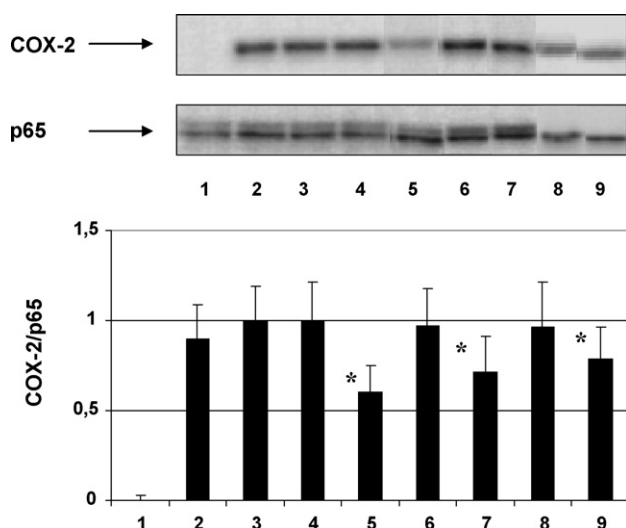


Fig. 9. *In vitro* inhibition of COX-2 by PNAs microsphere complexes. Above: immunoblot analysis of COX-2 expression levels in murine macrophages. Lane 1: unstimulated macrophages. Lanes 2–9: macrophages stimulated with LPS and treated with nude microsphere HID4 (lane 3), scramble-A25, -S3 or -L205/microsphere complexes (lanes 4, 6 and 8, respectively), antisense KKK-A25, -S3 and -L205 microsphere complexes (lanes 5, 7 and 9). Blots were probed with anti-COX-2, anti-p65 (Rel A) antibodies. Below: quantification by laser densitometry of COX-2 levels normalized to p65 (Rel A) and expressed as COX-2/p65 ratio. Results are the mean of three different experiments \pm S.D. * $p < 0.00003$ compared to lane 3.

administered dose. In agreement with PMMA biocompatibility, the described polymeric microspheres did not show any toxicity in murine macrophages neither free or complexed with PNAs.

The efficacy of PNA/microsphere complexes was tested in vitro in cultured macrophages and compared to the activity of control scramble sequences as well as of a specific inhibitor of COX-2 (NS398). All lysine modified PNAs adsorbed on polymeric core-shell microspheres were shown to be able to specifically inhibit COX-2 protein expression in macrophages with good efficiency at very low doses. In the described cellular model, the maximum inhibition efficiency (52%) was reached only with 100 μ M concentration of NS398 (data not shown), a well known specific inhibitor of COX-2 that is not specific for the macrophage cellular model. Instead, in the case of PNA/microsphere complexes, the maximum inhibition efficiency (40%) was reached with KKK-S3 antisense PNA bound to H1D4 microspheres (loading = 17.8 μ g/mg) which corresponds to an active concentration in the culture medium of about 37 nM. KKK-A25 and KKK-L205 antisense PNA sequences, delivered through polymeric microspheres, showed similar specific inhibition at 39 and 12 nM concentration, respectively. To our knowledge, these doses are significantly lower than those reported up to now for PNA antisense in vitro activity (Koppelhus and Nielsen, 2003).

5. Conclusion

PNA derivatization with basic aminoacids (KKK) allows their specific adsorption onto functional anionic core-shell polymeric microspheres, giving rise to ionic complex which are easy to prepare, to store and that are very stable in physiological buffers. To test their efficacy in vitro, we have studied the inhibition of the expression and activity of COX-2 protein after stimulation with LPS, in murine macrophages where an inhibition of the inflammatory response mediated by prostaglandins release can be obtained and measured. These polymeric carriers are efficiently phagocytosed by murine macrophages and able to release biologically active antisense PNAs inside cells where they can efficiently inhibit inducible protein expression at nanomolar concentration.

Scramble PNA failed to inhibit protein expression whereas NS398 inhibitor allowed comparable inhibition efficiency but only at 100 μ M concentration. Probably, delivery through microspheres allows PNA crossing of intact macrophage membrane, thus increasing their bioavailability inside cells. Preliminary results also indicate that this delivery system can even be more effective in vivo, thus representing a promising technology for improving PNA therapeutic applications. Antisense approach against COX-2 mRNA could effectively represent a good alternative to the drugs currently used in inflammatory diseases, which are affected by problems of toxicity, side effects and low specificity.

Acknowledgements

We are grateful to Marco Serra and Valentina Scopece for their enthusiastic collaboration during their stage for the achieve-

ment of the European degree in Pharmaceutical Sciences and to Dr. E. Pantucci for helpful technical assistance. We also thank Mara Mancini for her secretarial assistance.

References

- Albertshofer, K., Siwkowski, A.M., Wancewicz, E.V., Esau, C.C., Watanabe, T., Nishihara, K.C., Kinberger, G.A., Malik, L., Eldrup, A.B., Manoharan, M., Geary, R.S., Monia, B.P., Swayze, E.E., Griffey, R.H., Bennett, C.F., Maier, M.A., 2005. Structure–activity relationship study on a simple cationic peptide motif for cellular delivery of antisense peptide nucleic acid. *J. Med. Chem.* 48, 6741–6749.
- Caputo, A., Brocca-Cofano, E., Castaldello, A., De Michele, R., Altavilla, G., Marchisio, M., Gavioli, R., Rolen, U., Chiarantini, L., Cerasi, A., Dominici, S., Magnani, M., Cafaro, A., Sparnacci, K., Laus, M., Tondelli, L., Ensoli, B., 2004. Novel biocompatible anionic polymeric microspheres for the delivery of the HIV-1 Tat protein for vaccine application. *Vaccine* 22, 2910–2924.
- Chiarantini, L., Cerasi, A., Fraternali, A., Andreoni, F., Scarfi, S., Giovine, M., Clavarino, E., Magnani, M., 2002. Inhibition of macrophage iNOS by selective targeting of antisense PNA. *Biochemistry* 41, 8471–8477.
- Chiarantini, L., Cerasi, A., Millo, E., Benatti, U., Laus, M., Sparnacci, K., Magnani, L., Tondelli, L., 2005a. Antisense peptide nucleic acid delivered by core-shell microspheres. *J. Control. Release* 101, 397–398.
- Chiarantini, L., Cerasi, A., Fraternali, A., Millo, E., Benatti, U., Sparnacci, K., Laus, M., Ballestri, M., Tondelli, L., 2005b. Comparison of novel delivery systems for antisense peptide nucleic acids. *J. Control. Release* 109, 24–36.
- Christensen, L., Fitzpatrick, R., Gildea, B., Petersen, K.H., Hansen, H.F., Koch, T., Egholm, M., Buchardt, O., Nielsen, P.E., Coull, J., Berg, R.H., 1995. Solid-phase synthesis of peptide nucleic acids. *J. Peptide Sci.* 3, 175–183.
- Crofford, L.J., Wilder, R.L., Ristimaki, A.P., Sano, H., Remmers, E.F., Epps, H.R., Hla, T., 1994. *J. Clin. Invest.* 93, 1095–1101.
- Demidov, V.V., Potaman, V.N., Frank-Kamenetskii, M.D., Egholm, M., Buchardt, O., Sonnichsen, S.H., Nielsen, P.E., 1994. Stability of peptide nucleic acids in human serum and cellular extracts. *Biochem. Pharmacol.* 48, 1310–1313.
- Dubois, R.N., Abramson, S.B., Crofford, L., Gupta, R.A., Simon, L.S., Van de Putte, L.B., Lipsky, P.E., 1998. Cyclooxygenase in biology and disease. *FASEB J.* 12, 1063–1073.
- Ensoli, B., Caputo, A., Laus, M., Tondelli, L., Sparnacci, K., 2004. Nanoparticles for delivery of a pharmacologically active agent, PCT/EP 2004/012420.
- Faruqi, A.F., Egholm, M., Glazer, P.M., 1998. Peptide nucleic acid-targeted mutagenesis of a chromosomal gene in mouse cells. *Proc. Natl. Acad. Sci. U.S.A.* 95, 1398–1403.
- Hamilton, S.E., 1996. Specific and nonspecific inhibition of transcription by DNA, PNA, and phosphorothioate promoter analog duplexes. *Bioorg. Med. Chem. Lett.* 6, 2897–2900.
- Hamilton, S.E., Simmons, C.G., Kathiriya, I.S., Corey, D.R., 1999. Cellular delivery of peptide nucleic acids and inhibition of human telomerase. *Chem. Biol.* 6, 343–351.
- Hida, T., Yatabe, Y., Achiwa, H., Muramatsu, H., Kozaki, K., Nakamura, S., Ogawa, M., Mitsudomi, T., Sugiura, T., Takahashi, T., 1998. Increased expression of cyclooxygenase-2 occurs frequently in human lung cancers, specifically in adenocarcinoma. *Cancer Res.* 58, 3761–3764.
- Koppelhus, U., Awasthi, S.K., Zachar, V., Holst, H.U., Ebbesen, P., Nielsen, P.E., 2002. Cell-dependent differential cellular uptake of PNA, peptides and PNA-peptide conjugates. *Antisense Nucl. Acid Drug Dev.* 12, 51–63.
- Koppelhus, U., Nielsen, P.E., 2003. Cellular delivery of peptide nucleic acid (PNA). *Adv. Drug Deliv. Rev.* 55, 267–280.
- Leung, W.K., To, K.F., Go, M.Y.Y., Chan, K.K., Chan, F.K.L., Ng, E.K.W., Chung, S.C.S., Sung, J.J.Y., 2003. Cyclooxygenase-2 upregulates vascular endothelial growth factor expression and angiogenesis in human gastric carcinoma. *Int. J. Oncol.* 23, 1317–1322.
- Lowry, O.H., Rosebrough, N.J., Farr, A.L., Randall, R.J., 1951. Protein measurement with the folin phenol agent. *J. Biol. Chem.* 193, 265–275.
- Nielsen, P.E., Egholm, M., Berg, R.H., Buchardt, O., 1991. Sequence-selective recognition of DNA by strand displacement with a thymine-substituted polyamide. *Science* 254, 1497–1500.

- Putnam, D.A., 1996. Antisense strategies and therapeutic applications. *Am. J. Health Syst. Pharm.* 53, 151–160.
- Rapozzi, V., Burn, B.E.A., Cogoi, S., van der Marel, G., van Boom, J.H., Quadri-foglio, F., Xodo, L.E., 2002. Antiproliferative effect in chronic myeloid leukaemia cells by antisense peptide nucleic acids. *Nucl. Acids Res.* 30, 3712–3721.
- Riccio, M., Di Giaimo, R., Pianetti, S., Palmieri, P.P., Melli, M., Santi, S., 2001. Nuclear localization of cystatin B, the cathepsin inhibitor implicated in myoclonus epilepsy (EPM1). *Exp. Cell Res.* 262, 84–94.
- Sazani, P., Kang, S.H., Maier, M.A., Wei, C., Dillman, J., Summerton, J., Manoharan, M., Kole, R., 2001. Nuclear antisense effects of neutral, anionic and cationic oligonucleotide analogs. *Nucl. Acids Res.* 29, 3965–3974.
- Sazani, P., Gemignani, F., Kang, S.H., Maier, M.A., Manoharan, M., Persmark, M., Bortner, D., Kole, R., 2002. Systemically delivered antisense oligomers upregulate gene expression in mouse tissues. *Nat. Biotechnol.* 20, 1228–1233.
- Scarfì, S., Gasparini, A., Damonte, G., Benatti, U., 1997. Synthesis, uptake, and intracellular metabolism of a hydrophobic tetrapeptide-peptide nucleic acid (PNA)-biotin molecule. *Biochem. Biophys. Res. Commun.* 236, 323–326.
- Scarfì, S., Giovine, M., Pintus, R., Millo, E., Clavarino, E., Pozzolini, M., Sturla, L., Stock, R.P., Benatti, U., Damonte, G., 2003. Selective inhibition of inducible cyclo-oxygenase-2 expression by antisense peptide nucleic acids in intact murine macrophages. *Biotech. Appl. Biochem.* 38, 61–69.
- Shammas, M.A., Simmons, C.G., Corey, D.R., Shmookler Reis, R.J., 1999. Telomerase inhibition by peptide nucleic acids reverses ‘immortality’ of transformed human cells. *Oncogene* 18, 6191–6200.
- Sheehan, K.M., Sheahan, K., O’Donoghue, D.P., MacSweeney, F., Conroy, R.M., Fitzgerald, D.J., Murray, F.E., 1999. The relationship between cyclooxygenase 2 expression and colorectal cancer. *J. Am. Med. Assoc.* 282, 1254–1257.
- Smalley, W., DuBios, R.N., 1997. Colorectal cancer and nonsteroidal anti-inflammatory drug. *Adv. Pharmacol.* 39, 1–20.
- Smith, W.L., Garavito, R.M., DeWitt, D.L., 1996. Prostaglandin endoperoxide H synthases (cyclooxygenases)-1 and -2. *J. Biol. Chem.* 271, 33157–33160.
- Sparnacci, K., Laus, M., Tondelli, L., Bernardi, C., Magnani, L., Corticelli, F., Marchisio, M., Ensoli, B., Castaldello, A., Caputo, A., 2005. Protein friendly core-shell microspheres by dispersion polymerization as promising delivery systems for protein-based vaccines. *J. Biomater. Sci.* 16, 1557–1574.
- Tondelli, L., Ricca, A., Laus, M., Lelli, M., Citro, G., 1998. Highly efficient cellular uptake of c-myc antisense oligonucleotides through specifically designed polymeric nanospheres. *Nucl. Acids Res.* 26, 5425–5431.
- Turner, J.J., Ivanova, G.D., Verbeure, B., Williams, D., Arzumanov, A.A., Abes, S., Lebleu, B., Gait, M.J., 2005. Cell-penetrating peptide conjugates of peptide nucleic acids (PNA) as inhibitors of HIV-1 Tat-dependent trans-activation in cells. *Nucl. Acids Res.* 33, 6837–6849.
- Vane, J.R., Bakhle, Y.S., Botting, R.M., 1998. Cyclooxygenase 1 and 2. *Annu. Rev. Pharmacol. Toxicol.* 38, 97–120.